Whole-lifetime Coordinated Service Strategy for Battery Energy Storage System Considering Multi-stage Battery Aging Characteristics

Feilong Fan, *Member*, *IEEE*, Yan Xu, *Senior Member*, *IEEE*, Rui Zhang, *Member*, *IEEE*, and Tong Wan

***Abstract*—One battery energy storage system (BESS) can be used to provide different services, such as energy arbitrage (EA) and frequency regulation (FR) support, etc., which have different revenues and lead to different battery degradation profiles. This paper proposes a whole-lifetime coordinated service strategy to maximize the total operation profit of BESS. A multi-stage battery aging model is developed to characterize the battery aging rates during the whole lifetime. Considering the uncertainty of electricity price in EA service and frequency deviation in FR service, the whole problem is formulated as a two-stage stochastic programming problem. At the first stage, the optimal service switching scheme between the EA and FR services are formulated to maximize the expected value of the whole-lifetime operation profit. At the second stage, the output power of BESS in EA service is optimized according to the electricity price in the hourly timescale, whereas the output power of BESS in FR service is directly determined according to the frequency deviation in the second timescale. The above optimization problem is then converted as a deterministic mixed-integer nonlinear programming (MINLP) model with bilinear items. McCormick envelopes and a bound tightening algorithm are used to solve it. Numerical simulation is carried out to validate the effectiveness and advantages of the proposed strategy.**

***Index Terms*—Battery energy storage system (BESS), whole-lifetime coordinated service, multi-stage battery aging model, two-stage stochastic programming, mixed-integer nonlinear programming (MINLP).**

NOMENCLATURE

A. Indices

i, l	Indices of typical service period and life stage
$i_{\max}$, $l_{\max}$	The maximum indices of typical service period and life stage
t_{EA}, t_{FR}	Indices of time intervals in energy arbitrage (EA) and frequency regulation (FR) services
$t_{\mathrm{EA}}^{\max}$, $t_{\mathrm{FR}}^{\max}$	The maximum indices of time intervals in EA and FR services

B. Parameters

η_{c}, η_{d}	Charging and discharging efficiencies of battery energy storage system (BESS)
κ_{D}	Linearized cyclic aging rate corresponding to unit cycle depth
κ_{cal}	Linearized calendar aging rate corresponding to unit operation time
κ_1^{D}	Cyclic aging rate corresponding to unit cycle depth at life stage 1
κ_1^{cal}	Calendar aging rate corresponding to unit operation time at life stage 1
χ_l	Calendar accelerating factor at life stage l
ρ_k	Possibility of the second-stage scenario
$\pi_u^{\min}$, $\pi_u^{\max}$	The minimum and maximum values of variable π_u
$\omega_u^{\min}$, $\omega_u^{\max}$	The minimum and maximum values of variable ω_u
Δf_0, Δf_1	Bound of dead band and the maximum tolerant frequency deviation in FR service
$\Delta\hat{f}_{l,t_{\mathrm{FR}}}$	Frequency deviation
Δt_{EA}, Δt_{FR}	Time spans of intervals in EA and FR services
Δt	Length of a time interval
$a_{m_\rho,l}$, $b_{m_\rho,l}$	Parameters in piecewise linear calculation function for cyclic accelerating factor due to charging-discharging rate at segment m_ρ and life stage l
$C_{\mathrm{op,u}}$	Maintenance cost of BESS in unit operation time
$E_{\max}$	The maximum rated energy capacity
$E^{\mathrm{EA,min}}$, $E^{\mathrm{EA,max}}$	The minimum and maximum values for stored energy of BESS in EA service
$L_{l,i}^{\mathrm{stage}}$, $L_i^{\mathrm{s,max}}$	Life loss limitation for BESS at life stage l and whole lifetime
$P_{l,t_{\mathrm{FR}}}^{\mathrm{FR,max}}$,	The maximum and minimum power in FR ser-

Manuscript received: January 15, 2021; revised: June 9, 2021; accepted: September 7, 2021. Date of CrossCheck: September 7, 2021. Date of online publication: November 1, 2021.

This work was partially supported by T-RECs Energy Pte. Ltd. under project (No. 04IDS000719N014).

This article is distributed under the terms of the Creative Commons Attribution 4.0 International License (http://creativecommons.org/licenses/by/4.0/).

F. Fan is with the Energy Research Institute @ NTU, Nanyang Technological University, Singapore, and he is also with the College of Smart Energy, Shanghai Jiao Tong University, Shanghai, China (e-mail: feilong_fan@163.com).

Y. Xu is with School of Electrical and Electronic Engineering, Nanyang Technological University, Singapore (e-mail: eeyanxu@gmail.com).

R. Zhang (corresponding author) is with The University of New South Wales, Sydney, Australia (e-mail: rachelzhang.au@gmail.com).

T. Wan is with University of Sydney, Sydney, Australia (e-mail: tong.wan@sydney.edu.au).

DOI: 10.35833/MPCE.2021.000034

$P_{l,t_{\mathrm{FR}}}^{\mathrm{FR,min}}$ vice

$P_{l,t_{\mathrm{EA}}}^{\mathrm{EA,ch,max}}$, $P_{l,t_{\mathrm{EA}}}^{\mathrm{EA,dh,max}}$ The maximum charging and discharging power of BESS in EA service

P_{rated} Rated charging-discharging power

$r_{\mathrm{reserve}}^{\mathrm{FR}}$, $P_{\mathrm{reserve}}^{\mathrm{FR}}$ Reserve price and reserve power in FR service

$r_{t_{\mathrm{EA}}}^{\mathrm{EA}}$ Hourly electricity price in EA service

r_{d} Discount rate

$\hat{t}_i^{\mathrm{Y}}$ Time length of whole service period

C. Variables

α_i Binary variable that decides time span of whole service period

$\beta_{l,i}^{\mathrm{EA}}$, $\beta_{l,i}^{\mathrm{FR}}$ Binary variables that limit time spans of EA and FR services at life stage l

$\beta_{l,i}^{\mathrm{com}}$ Binary variable that limits life loss for BESS at life stage l

π_u, ω_u Variables in McCormick envelopes

$E_{l,t_{\mathrm{EA}},i}^{\mathrm{EA}}$ Stored energy of BESS at life stage l in EA service

G_l^{EA}, G^{FR} Revenues of BESS in EA and FR services

$g(\boldsymbol{y})$ The second-stage optimization problem

L^{cyc} Linearized cyclic aging rate

L_D^{cyc}, $L_{S^{\mathrm{m}}}^{\mathrm{cyc}}$, L_T^{cyc} Linearized cyclic aging coefficients due to cycle depth, mean state-of-charge (SOC), and temperature

L^{cal} Linearized calendar aging rate

$L_{\Delta t}^{\mathrm{cal}}$, $L_{S^i}^{\mathrm{cal}}$, L_T^{cal} Linearized calendar aging coefficients due to operation time, initial SOC, and temperature

L^{com} Comprehensive linearized aging rate

$L_l^{\mathrm{cyc,m}}$ Multi-stage cyclic aging rate at life stage l

$L_{\rho_{\mathrm{c}},l}^{\mathrm{rate}}$ Cyclic accelerating factor due to charging-discharging rate at life stage l

$L_l^{\mathrm{cal,m}}$ Multi-stage calendar aging rate at life stage l

$L_l^{\mathrm{com,m}}$ Comprehensive multi-stage aging rate at life stage l

$L_{l,t_{\mathrm{EA}},i}^{\mathrm{EA,ch}}$, $L_{l,t_{\mathrm{EA}},i}^{\mathrm{EA,dh}}$, $\hat{L}_{l,t_{\mathrm{FR}}}^{\mathrm{FR,ch}}$, $\hat{L}_{l,t_{\mathrm{FR}}}^{\mathrm{FR,dh}}$ Aging rates during charging and discharging stages in EA and FR services at life stage l

$P_{t_{\mathrm{EA}}}^{\mathrm{EA}}$ Output power of BESS in EA service

P^{ec}, P^{ed} Charging and discharging power for battery ($P^{\mathrm{ec}} \geq 0$, $P^{\mathrm{ed}} \geq 0$)

$P_{l,t_{\mathrm{EA}},i}^{\mathrm{EA,ch}}$, $P_{l,t_{\mathrm{EA}},i}^{\mathrm{EA,dh}}$, $\hat{P}_{l,t_{\mathrm{FR}}}^{\mathrm{FR,ch}}$, $\hat{P}_{l,t_{\mathrm{FR}}}^{\mathrm{FR,dh}}$ Charging and discharging power of BESS in EA and FR services at life stage l

$Q(\boldsymbol{x},\boldsymbol{\xi})$ Optimal value of the second-stage problem

t_{si} Time of service switching point

$t_i^{\mathrm{d,max}}$ Time span of whole operation period

$t_{l,i}^{\mathrm{d,EA}}$, $t_{l,i}^{\mathrm{d,FR}}$ Time spans of EA and FR services at life stage l

D. Vectors and Sets

$\boldsymbol{\xi}$, $\boldsymbol{\xi}_k$ Random vectors in the second-stage optimization and scenario k

$\Omega(\boldsymbol{x},\boldsymbol{\xi})$ The second-stage constraint set

$F, f(\boldsymbol{x})$ Constraint set and optimization problem

$\boldsymbol{x}$ Vector for variables in the first-stage decision

$\boldsymbol{y}$, $\boldsymbol{y}_k$ Vectors for variables in the second-stage decision and scenario k

I. Introduction

ENERGY storages are promising facilities to improve the robustness, resiliency, and efficiency of modern power systems and cope with the challenges brought by growing penetration of uncertain and intermittent renewable resources [1]. An energy storage can store excess energy during periods of high power generation and inject the stored energy during peak load periods. As a result, renewable generation curtailment can be reduced, and expensive fast generating units can be avoided [2]. Studies suggest that the required power capacity of energy storages in the United States will be as high as 152 GW by 2050 [3]. Much of this capacity is expected to be achieved by battery energy storage systems (BESSs), which have rapid ramp rate [4] and fast response speed [5]. As the capital costs of the BESSs are quite high, maximizing the economic benefits for BESSs is the main objective of the operation strategies in most services, such as energy arbitrage (EA), frequency regulation (FR), and peak shaving.

EA and FR are two main services for the BESSs. In EA service, BESSs operate according to the electricity price in hourly timescale [6]. A dynamic programming approach considering cycle aging and price uncertainty is proposed in [7] to maximize the income of the BESS. A stochastic optimization model is formulated in [8] to maximize the profit of BESS under the uncertainty of the day-ahead and real-time electricity prices. In FR service, BESSs aim to decrease the frequency deviation in a short time interval. An optimal control and bidding policy based on realistic market settings and an accurate battery aging model are adopted in [9] to maximize the market profits while satisfying the performance requirement of FR market. A real-time greedy-index dispatching policy is developed in [10] to use electric vehicle battery for power system frequency support. Due to the different charging/discharging depth and frequency, the battery lifetime degradation in different services is different. According to existing studies, BESSs in EA service have lower life degradations, whereas those in FR service have higher revenues [11]. Considering different degradation properties and revenues of a BESS in different services, co-optimization of a BESS for both EA and FR services has the potential to increase the total profit, which can be calculated as the stacked value of the profits from different services.

Co-optimization strategies can be classified into two main categories: short-term joint-service optimization and long-term service-switching optimization. The short-term joint-service optimization is usually used in the daily operation of a BESS, whereas the long-term service-switching optimization is mostly considered in the whole-lifetime service. A robust optimization model is formulated in [12] to maximize the profit of a BESS in joint energy and ancillary services. A

joint stochastic optimization model considering super-linear gains is proposed in [13] to coordinate the operation of a BESS in peak shaving and FR services. A multi-scale dynamic programming method is proposed in [14] to co-optimize the performance of a BESS in joint EA and FR services. An optimal dispatch strategy is proposed in [15] to co-optimize the performance of a battery energy storage station in voltage distribution improvement and peak load shifting. The above works aim to maximize the short-term profit by co-optimizing the participation strategy for the BESS to provide both services at the same time. However, when both services are provided simultaneously, the BESS cannot provide reliable FR service to the grid, which brings high risk to the operation of the whole system. Especially when the electricity price in EA service reaches the maximum or the minimum value, the BESSs will be charged/discharged at the maximum power and cannot provide reserve power for FR [16]. In the practical application, most power systems need to contract with some providers to have reliable FR services on standby and have strict rules to guarantee high-quality performance of these BESSs [17]. Those strict rules forbid the BESSs to provide both services simultaneously [16]. On the other hand, a long-term service-switching strategy is proposed in [18] to maximize the whole-lifetime profit by switching the service from FR to EA at a certain state of health (SOH) of the battery. However, the method in [18] is on the basis of one-off switching, which cannot fully use the battery for the maximum revenue at different SOHs.

Aging characteristics significantly impact the economic benefit of a BESS [19], [20]. In [12] and [14], battery aging characteristics are not considered in the co-optimization. A linearized cycle-depth stressed aging function is used in [13] to evaluate the lifetime degradation of a battery. An exponential aging model considering cycle number and cycle depth is used in [18] to maximize the whole-lifetime profit. The above-mentioned co-optimization strategies only consider the external impacts on the battery aging process. The battery aging characteristics due to the internal chemical reaction process are ignored. Due to the solid-electrolyte-interphase (SEI) formation, the aging rate of the lithium-ion battery is not a linear process [21]. A two-exponential function is used in [22] to model the nonlinear degradation progress of the battery. One exponential portion is used to calculate the aging rate due to internal SEI formation process. Another exponential portion is used to calculate the aging rate due to external impacts from cycle depth, operation time, state-of-charge (SOC), and temperature. However, the two-exponential function is highly nonlinear and too complicated to be applied in a long-term optimization.

This paper focuses on the whole-lifetime coordinated service over the long-term horizon. The contributions of this paper are as follows.

1) A whole-lifetime coordinated service strategy is proposed to maximize the whole-lifetime operation profit for a BESS by switching the service between EA and FR at proper SOHs.

2) A comprehensive multi-stage aging model is established to calculate the aging rate of a BESS considering both external impacts and internal chemical reaction process.

3) A two-stage stochastic programming model is formulated to model the optimization problem. At the first stage, the optimal service switching scheme between the EA and FR services are formulated to maximize the expected value of the whole-lifetime operation profit. At the second stage, the output power of BESS in EA service is optimized according to the electricity price in the hourly timescale, whereas the output power of BESS in FR service is directly determined according to the frequency deviation in the second timescale. McCormick envelopes and a bound tightening algorithm are used to solve the model.

The remainder of this paper is organized as follows. Section II introduces the framework of whole-lifetime coordinated service strategy. Section III illustrates the multi-stage battery aging model. In Section IV, the mathematical formulation is presented. The solution method is developed in Section V. The effectiveness of the proposed strategy is validated in Section VI. Finally, Section VII provides the conclusion.

II. Whole-Lifetime Coordinated Service Strategy

A. Overview of Whole-lifetime Coordinated Service Strategy

The proposed whole-lifetime coordinated service strategy aims to maximize the total operation profit of a BESS through switching the service at proper SOHs. The operation revenues and costs are settled at the end of whole service period. An overview of the proposed strategy is shown in Fig. 1.

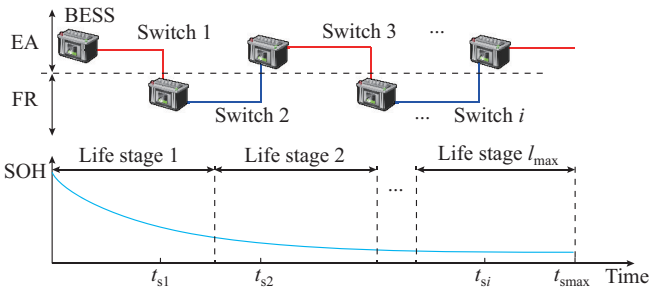

Fig. 1. Overview of whole-lifetime coordinated service strategy.

Figure 1 outlines the main idea of the proposed strategy. At the first stage, a new BESS can provide either EA or FR service. When the SOH shrinks to a certain threshold, the BESS switches the service to maximize the whole-lifetime operation profit. More than one service switches can be made during the whole operation period. At the second stage, based on the service switching decision, the battery output power is formulated according to the operation rule in each service.

B. Operation Rule in EA Service

A BESS can provide EA service either as a seller or a buyer according to the hourly electricity price [18]. When the electricity price is low, the BESS is charged to decrease the cost of storing energy. When the electricity price is high, the BESS is discharged to gain more revenues using the

stored energy [23]. The daily revenue for the BESS in EA service can be calculated as:

$$G_l^{\mathrm{EA}} = \sum_{t_{\mathrm{EA}}=1}^{t_{\mathrm{EA}}^{\max}} r_{t_{\mathrm{EA}}}^{\mathrm{EA}} \left(P_{l,t_{\mathrm{EA}}}^{\mathrm{EA,dh}} - P_{l,t_{\mathrm{EA}}}^{\mathrm{EA,ch}} \right) \Delta t_{\mathrm{EA}} \tag{1}$$

C. Operation Rule in FR Service

A BESS can be used to provide FR services in the short timescale. The operation rule in FR service [24] is given as:

$$\hat{P}_{l,t_{\mathrm{FR}}}^{\mathrm{FR}} = \begin{cases} \min\left\{ P_{l,t_{\mathrm{FR}}}^{\mathrm{FR,max}}, P_{\mathrm{reserve}}^{\mathrm{FR}}, P_{\mathrm{reserve}}^{\mathrm{FR}} \dfrac{\Delta\hat{f}_{l,t_{\mathrm{FR}}} - \Delta f_0}{\Delta f_1 - \Delta f_0} \right\} & \Delta\hat{f}_{l,t_{\mathrm{FR}}} \in [\Delta f_0, +\infty) \\ 0 & \Delta\hat{f}_{l,t_{\mathrm{FR}}} \in (-\Delta f_0, \Delta f_0) \\ \max\left\{ P_{l,t_{\mathrm{FR}}}^{\mathrm{FR,min}}, P_{\mathrm{reserve}}^{\mathrm{FR}}, P_{\mathrm{reserve}}^{\mathrm{FR}} \dfrac{\Delta\hat{f}_{l,t_{\mathrm{FR}}} + \Delta f_0}{\Delta f_1 - \Delta f_0} \right\} & \Delta\hat{f}_{l,t_{\mathrm{FR}}} \in (-\infty, -\Delta f_0] \end{cases} \tag{2}$$

According to (2), a dead-band of $(-\Delta f_0, \Delta f_0)$ is set for the BESS to avoid unnecessary frequent usage. When the frequency deviation is in $(-\infty, -\Delta f_0] \cup [\Delta f_0, +\infty)$, the output of BESS is increased linearly and limited by the reserve power and the maximum and minimum power values. When the power is positive, the BESS is charged. When the power is negative, the BESS is discharged. During each period in FR service, the BESS operates according to the operation rules and real-time power demand for 900 s, after which a break of 900 s is permitted to recover the SOC to the initial value.

The FR service considered in this paper is a reliable FR service with fixed standby capacity. According to the European FR market, the BESS in reliable FR service is paid by the system operator (SO) with a fixed price for reserve power [18]. Considering that the BESS provides FR service at the first half of each interval, the daily revenue in the FR service is calculated as:

$$G^{\mathrm{FR}} = \frac{1}{2} \sum_{t_{\mathrm{FR}}=1}^{t_{\mathrm{FR}}^{\max}} r_{\mathrm{reserve}}^{\mathrm{FR}} P_{\mathrm{reserve}}^{\mathrm{FR}} \Delta t_{\mathrm{FR}} \tag{3}$$

III. Multi-stage Battery Aging Model

A. Degradation Mechanism

This paper considers the lithium-ion battery which is most widely adopted in practice. The formulation and growth of SEI cause the capacity loss of the lithium-ion batteries [25]. When a new battery starts to operate, a lot of active lithium ions are consumed to form the SEI film [26]. After a stable film is formed, the requirement of the active lithium ions to form the SEI film decreases. As a result, the aging rate at the early life stages is significantly higher than that at the later life stages. Then, when the battery reaches the end of life, there are few active lithium-ions left, and the aging rate increases rapidly [22]. Based on the testing data in [22] and [27], the degradation of a lithium-ion battery can be divided into different linearized life stages. Within each life stage, the aging rate can be formulated as a linearized function of cycle depth [13]. At different life stages, an accelerating factor can be multiplied to the linearized aging function to model the nonlinear aging characteristics.

In this work, lifetime loss is used to evaluate the aging rate L. When $L=0$, the lithium-ion battery has no lifetime loss. When $L=1$, the lithium-ion battery degrades from the beginning to the end of life. The end of life is typically defined as the point at which the battery only provides 80% of its rated maximum capacity.

B. Linearized Aging Model

A linearized aging model depending on the external stress factors is widely used to describe the aging characteristics of the battery. The linearized aging model considers the cyclic and calendar aging functions, which are described as follows.

1) Linearized Cyclic Aging Function

A linearized cyclic aging function [22], [27] is formulated to calculate the degradation of a BESS, as shown in (4).

$$L^{\mathrm{cyc}} = L_D^{\mathrm{cyc}} L_{S^{\mathrm{m}}}^{\mathrm{cyc}} L_T^{\mathrm{cyc}} \tag{4}$$

In (4), the linearized cyclic aging rate L^{cyc} is the product of aging coefficients corresponding to the cycle depth, mean SOC, and temperature, i.e., L_D^{cyc}, $L_{S^{\mathrm{m}}}^{\mathrm{cyc}}$, and L_T^{cyc}, respectively. In the application of above linearized aging function, the aging coefficients due to mean SOC and temperature are usually regarded as constant parameters. The cyclic aging rate is commonly fitted as a linear function of cycle depth. As the cycle depth is a linear function of charging-discharging power, the linearized cyclic aging rate can be calculated as a linear function of charging-discharging power [13], as shown in (5).

$$L^{\mathrm{cyc}} = \begin{cases} \dfrac{\kappa_{\mathrm{D}} \eta_{\mathrm{c}} P^{\mathrm{ec}} \Delta t}{E_{\max}} & \text{charging} \\ \dfrac{\kappa_{\mathrm{D}} P^{\mathrm{ed}} \Delta t}{\eta_{\mathrm{d}} E_{\max}} & \text{discharging} \end{cases} \tag{5}$$

2) Linearized Calendar Aging Function

A linearized calendar aging function [22], [28] is formulated to calculate the degradation of the BESS, as shown in (6).

$$L^{\mathrm{cal}} = L_{\Delta t}^{\mathrm{cal}} L_{S^i}^{\mathrm{cal}} L_T^{\mathrm{cal}} \tag{6}$$

In (6), the calendar aging rate L^{cal} is the product of aging coefficients corresponding to operation time, initial SOC, and temperature, i.e., $L_{\Delta t}^{\mathrm{cal}}$, $L_{S^i}^{\mathrm{cal}}$, and L_T^{cal}, respectively. As the temperature of the BESS can be well controlled by the cooling system and the initial and final SOCs in this paper are all 50%, the aging coefficients due to the impacts of initial SOCs and temperature are regarded as constant parameters. Then, the calendar aging rate can be calculated as a linear function of stored time [28] in (7).

$$L^{\mathrm{cal}} = \kappa_{\mathrm{cal}} \Delta t \tag{7}$$

3) Comprehensive Linearized Aging Function

According to the functions in (5) and (7), the comprehensive linearized aging function is expressed as:

$$L^{\mathrm{com}}=\begin{cases}\dfrac{\kappa_{\mathrm{D}}\eta_{\mathrm{c}}P^{\mathrm{ec}}\Delta t}{E_{\max}}+\kappa_{\mathrm{cal}}\Delta t & \text{charging}\\ \dfrac{\kappa_{\mathrm{D}}P^{\mathrm{ed}}\Delta t}{\eta_{\mathrm{d}}E_{\max}}+\kappa_{\mathrm{cal}}\Delta t & \text{discharging}\end{cases} \tag{8}$$

C. Multi-stage Aging Model

The aging rate of a BESS depends on not only the external stress factors but also on its internal chemical reaction process. A multi-stage aging model is formulated to show the comprehensive aging characteristics.

1) Multi-stage Cyclic Aging Function

Multi-stage cyclic aging rates are calculated according to the accelerating factors corresponding to the charging-discharging rates at different life stages, which is expressed as:

$$L_l^{\mathrm{cyc,m}}=L_1^{\mathrm{cyc,m}}L_{\rho_{\mathrm{e}},l}^{\mathrm{rate}} \tag{9}$$

where $L_1^{\mathrm{cyc,m}}$ is calculated in (5) by replacing κ_{D} with κ_1^{D}; and $L_{\rho_{\mathrm{e}},l}^{\mathrm{rate}}$ is calculated by:

$$L_{\rho_{\mathrm{e}},l}^{\mathrm{rate}}=a_{m_\rho,l}\rho^{\mathrm{e}}+b_{m_\rho,l}\qquad \rho^{\mathrm{e}}\in[\rho_{m_\rho,l},\rho_{m_\rho+1,l}] \tag{10}$$

The charging-discharging rate ρ^{e} is defined as the ratio of the charging-discharging power to rated power. Then, the multi-stage cyclic aging rate can be calculated as:

$$L_l^{\mathrm{cyc,m}}=\begin{cases}\dfrac{\kappa_1^{\mathrm{D}}\eta_{\mathrm{c}}P^{\mathrm{ec}}\Delta t}{E_{\max}}\left(a_{m_\rho,l}\dfrac{P^{\mathrm{ec}}}{P_{\mathrm{rated}}}+b_{m_\rho,l}\right) & \text{charging}\\ \dfrac{\kappa_1^{\mathrm{D}}P^{\mathrm{ed}}\Delta t}{\eta_{\mathrm{d}}E_{\max}}\left(a_{m_\rho,l}\dfrac{P^{\mathrm{ed}}}{P_{\mathrm{rated}}}+b_{m_\rho,l}\right) & \text{discharging}\end{cases} \tag{11}$$

2) Multi-stage Calendar Aging Function

Multi-stage calendar aging rates are calculated according to the accelerating factors corresponding to different life stages in (12).

$$L_l^{\mathrm{cal,m}}=\chi_l L_1^{\mathrm{cal,m}} \tag{12}$$

where $L_1^{\mathrm{cal,m}}$ is calculated in (7) by replacing κ_{cal} with κ_1^{cal}.

Then, the multi-stage calendar aging function is shown as:

$$L_l^{\mathrm{cal,m}}=\chi_l\kappa_1^{\mathrm{cal}}\Delta t \tag{13}$$

3) Comprehensive Multi-stage Aging Function

Based on the multi-stage cyclic and calendar aging functions, the comprehensive multi-stage aging function is formulated as:

$$L_l^{\mathrm{com,m}}=\begin{cases}\dfrac{\kappa_1^{\mathrm{D}}\eta_{\mathrm{c}}P^{\mathrm{ec}}\Delta t}{E_{\max}}\left(a_{m_\rho,l}\dfrac{P^{\mathrm{ec}}}{P_{\mathrm{rated}}}+b_{m_\rho,l}\right)+\chi_l\kappa_1^{\mathrm{cal}}\Delta t & \text{charging}\\ \dfrac{\kappa_1^{\mathrm{D}}P^{\mathrm{ed}}\Delta t}{\eta_{\mathrm{d}}E_{\max}}\left(a_{m_\rho,l}\dfrac{P^{\mathrm{ed}}}{P_{\mathrm{rated}}}+b_{m_\rho,l}\right)+\chi_l\kappa_1^{\mathrm{cal}}\Delta t & \text{discharging}\end{cases} \tag{14}$$

IV. Mathematical Formulation

A. Optimization Model for Whole-lifetime Coordinated Service

The optimal whole-lifetime coordinated service strategy aims to maximize the whole-lifetime operation profit by switching the service at proper SOHs. The whole-lifetime operation profit is evaluated by the net present value (NPV) considering the revenues and costs during the whole service period. Decision variables are the selection for total service time, time spans of services at different life stages, and charging/discharging power for the BESS in EA and FR services. The mathematical model is formulated as:

$$\min\ \sum_{i=1}^{i_{\max}}\frac{1}{(1+r_{\mathrm{d}})^{\hat{t}_i^{\mathrm{Y}}}}\cdot \left[\underbrace{C_{\mathrm{op,u}}\sum_{l=1}^{l_{\max}}\left(t_{l,i}^{\mathrm{d,EA}}+t_{l,i}^{\mathrm{d,FR}}\right)}_{\text{Maintenance cost}}-\underbrace{\sum_{l=1}^{l_{\max}}t_{l,i}^{\mathrm{d,EA}}G_{l,i}^{\mathrm{EA}}+\sum_{l=1}^{l_{\max}}t_{l,i}^{\mathrm{d,FR}}G^{\mathrm{FR}}}_{\text{Operation revenue}}\right] \tag{15}$$

$$t_i^{\mathrm{d,max}}\le 365\sum_{i=1}^{i_{\max}}\alpha_i\hat{t}_i^{\mathrm{Y}}\quad\forall i \tag{16}$$

$$\sum_{i=1}^{i_{\max}}\alpha_i=1\quad\forall i \tag{17}$$

$$\sum_{l=1}^{l_{\max}}\left(t_{l,i}^{\mathrm{d,EA}}+t_{l,i}^{\mathrm{d,FR}}\right)=t_i^{\mathrm{d,max}}\quad\forall l,\forall i \tag{18}$$

$$0\le t_{l,i}^{\mathrm{d,EA}}\le\beta_{l,i}^{\mathrm{EA}}\hat{t}_{i_{\max}}^{\mathrm{Y}}\quad\forall l,\forall i \tag{19}$$

$$0\le t_{l,i}^{\mathrm{d,FR}}\le\beta_{l,i}^{\mathrm{FR}}\hat{t}_{i_{\max}}^{\mathrm{Y}}\quad\forall l,\forall i \tag{20}$$

$$E_{l,t_{\mathrm{EA}}+1,i}^{\mathrm{EA}}=E_{l,t_{\mathrm{EA}},i}^{\mathrm{EA}}+\eta_c P_{l,t_{\mathrm{EA}},i}^{\mathrm{EA,ch}}\Delta t_{\mathrm{EA}}-\frac{P_{l,t_{\mathrm{EA}},i}^{\mathrm{EA,dh}}\Delta t_{\mathrm{EA}}}{\eta_d}\quad\forall l,\forall t_{\mathrm{EA}},\forall i \tag{21}$$

$$E^{\mathrm{EA,min}}\le E_{l,t_{\mathrm{EA}},i}^{\mathrm{EA}}\le E^{\mathrm{EA,max}}\quad\forall l,\forall t_{\mathrm{EA}},\forall i \tag{22}$$

$$E_{l,1,i}^{\mathrm{EA}}=0.5E_{\max}\quad\forall l,\forall i \tag{23}$$

$$E_{l,t_{\mathrm{EA}}^{\max}+1,i}^{\mathrm{EA}}=0.5E_{\max}\quad\forall l,\forall i \tag{24}$$

$$0\le P_{l,t_{\mathrm{EA}},i}^{\mathrm{EA,ch}}\le\alpha_i P_{l,t_{\mathrm{EA}}}^{\mathrm{EA,ch,max}}\quad\forall l,\forall t_{\mathrm{EA}},\forall i \tag{25}$$

$$0\le P_{l,t_{\mathrm{EA}},i}^{\mathrm{EA,dh}}\le\alpha_i P_{l,t_{\mathrm{EA}}}^{\mathrm{EA,dh,max}}\quad\forall l,\forall t_{\mathrm{EA}},\forall i \tag{26}$$

$$\sum_{l=1}^{l_{\max}}\left[t_{l,i}^{\mathrm{d,EA}}\sum_{t_{\mathrm{EA}}=1}^{t_{\mathrm{EA}}^{\max}}\left(L_{l,t_{\mathrm{EA}},i}^{\mathrm{EA,ch}}+L_{l,t_{\mathrm{EA}},i}^{\mathrm{EA,dh}}\right)+t_{l,i}^{\mathrm{d,FR}}\sum_{t_{\mathrm{FR}}=1}^{t_{\mathrm{FR}}^{\max}}\left(\hat{L}_{l,t_{\mathrm{FR}}}^{\mathrm{FR,ch}}+\hat{L}_{l,t_{\mathrm{FR}}}^{\mathrm{FR,dh}}\right)\right]\le L_i^{\mathrm{s,max}}\quad\forall i \tag{27}$$

$$t_{l,i}^{\mathrm{d,EA}}\sum_{t_{\mathrm{EA}}=1}^{t_{\mathrm{EA}}^{\max}}\left(L_{l,t_{\mathrm{EA}},i}^{\mathrm{EA,ch}}+L_{l,t_{\mathrm{EA}},i}^{\mathrm{EA,dh}}\right)+t_{l,i}^{\mathrm{d,FR}}\sum_{t_{\mathrm{FR}}=1}^{t_{\mathrm{FR}}^{\max}}\left(\hat{L}_{l,t_{\mathrm{FR}}}^{\mathrm{FR,ch}}+\hat{L}_{l,t_{\mathrm{FR}}}^{\mathrm{FR,dh}}\right)\le\beta_{l,i}^{\mathrm{com}}L_{l,i}^{\mathrm{stage}}\quad\forall l,\forall i \tag{28}$$

$$t_{l,i}^{\mathrm{d,EA}}\sum_{t_{\mathrm{EA}}=1}^{t_{\mathrm{EA}}^{\max}}\left(L_{l,t_{\mathrm{EA}},i}^{\mathrm{EA,ch}}+L_{l,t_{\mathrm{EA}},i}^{\mathrm{EA,dh}}\right)+t_{l,i}^{\mathrm{d,FR}}\sum_{t_{\mathrm{FR}}=1}^{t_{\mathrm{FR}}^{\max}}\left(\hat{L}_{l,t_{\mathrm{FR}}}^{\mathrm{FR,ch}}+\hat{L}_{l,t_{\mathrm{FR}}}^{\mathrm{FR,dh}}\right)\ge\beta_{l+1,i}^{\mathrm{com}}L_{l,i}^{\mathrm{stage}}\quad\forall l\in[1,l_{\max}-1],\forall i \tag{29}$$

$$\beta_{l,i}^{\mathrm{com}}\ge\beta_{l+1,i}^{\mathrm{com}}\quad\forall l\in[1,l_{\max}-1],\forall i \tag{30}$$

$$\beta_{l,i}^{\mathrm{com}}\ge\beta_{l,i}^{\mathrm{EA}}\quad\forall l,\forall i \tag{31}$$

$$\beta_{l,i}^{\mathrm{com}}\ge\beta_{l,i}^{\mathrm{FR}}\quad\forall l,\forall i \tag{32}$$

$$\beta_{l,i}^{\mathrm{com}}\le\beta_{l,i}^{\mathrm{EA}}+\beta_{l,i}^{\mathrm{FR}}\quad\forall l,\forall i \tag{33}$$

The objective function in (15) consists of two parts: main-

tenance cost and operation revenue. Equation (16) shows that the time span of whole operation period should be limited by the time span of the whole service period. Equation (17) uses binary variables to decide the time span of the whole service period. Equation (18) indicates that the total time span of EA and FR services should be equal to that of the whole operation period. Equations (19) and (20) show the limits for the time spans of EA and FR services, respectively. Binary variables $\beta_{l,i}^{\mathrm{EA}}$ and $\beta_{l,i}^{\mathrm{FR}}$ are used to limit the time spans of EA and FR services at life stage l, respectively. Equation (21) calculates the stored energy of BESS. Equation (22) donates the minimum and maximum limits for the stored energy of BESS. Equations (23) and (24) show the initial and final values of the energy states for BESS in EA services, respectively. Equations (25) and (26) show that the power of BESS should be lower than the maximum charging and discharging power, respectively. Equations (27) and (28) are the limits for aging rates in the whole operation period and at each life stage, respectively. In (27) and (28), $L_{l,t_{\mathrm{EA}},i}^{\mathrm{EA,ch}}$ and $L_{l,t_{\mathrm{EA}},i}^{\mathrm{EA,dh}}$ can be calculated in (14) by replacing P^{ec} and P^{ed} with $P_{l,t_{\mathrm{EA}},i}^{\mathrm{EA,ch}}$ and $P_{l,t_{\mathrm{EA}},i}^{\mathrm{EA,dh}}$, respectively; $\hat{L}_{l,t_{\mathrm{FR}}}^{\mathrm{FR,ch}}$ and $\hat{L}_{l,t_{\mathrm{FR}}}^{\mathrm{FR,dh}}$ can be calculated in (14) by replacing P^{ec} and P^{ed} with $\hat{P}_{l,t_{\mathrm{FR}}}^{\mathrm{FR}}$ and $-\hat{P}_{l,t_{\mathrm{FR}}}^{\mathrm{FR}}$, respectively; and $\hat{P}_{l,t_{\mathrm{FR}}}^{\mathrm{FR}}$ can be calculated by the operation rule in (2). Equation (29) means that, if the useful lifetime at life stage $l+1$ is used in the operation period, the useful lifetime at life stage l should be fully used. Equation (30) means that, if $\beta_{l+1,i}^{\mathrm{com}}$ is equal to 1, $\beta_{l,i}^{\mathrm{com}}$ should be equal to 1. Equations (31)-(33) mean that, if $\beta_{l,i}^{\mathrm{EA}}$ or $\beta_{l,i}^{\mathrm{FR}}$ is equal to 1, $\beta_{l,i}^{\mathrm{com}}$ should be equal to 1. Constraints based on $\beta_{l,i}^{\mathrm{com}}$, $\beta_{l,i}^{\mathrm{EA}}$, and $\beta_{l,i}^{\mathrm{FR}}$ guarantee that the time spans of services at different life stages are formulated in a reasonable sequence.

B. Stochastic Programming Model

Considering the uncertainty of the electricity price in (1) and the frequency deviation in (2), a two-stage stochastic programming model is compactly formulated as:

$$\min_{\boldsymbol{x}\in F}\left\{f(\boldsymbol{x})+E(Q(\boldsymbol{x},\boldsymbol{\xi}))\right\} \tag{34}$$

where $f(\boldsymbol{x})$ is the first-stage problem, i.e., maintenance cost, and the first-stage decision vector $\boldsymbol{x}$ consists of the selection for total service time and time spans of services at all life stages; $Q(\boldsymbol{x},\boldsymbol{\xi})$ is the optimal value of the second-stage problem, i.e., the operation revenue $\min_{\boldsymbol{y}\in\Omega(\boldsymbol{x},\boldsymbol{\xi})} g(\boldsymbol{x},\boldsymbol{y})$, $\boldsymbol{y}$ is the second-stage decision vector, consisting of the charging/discharging power for the BESS in EA and FR services, and $\boldsymbol{\xi}$ is the random vector, which consists of the uncertain electricity price in EA service and uncertain frequency deviation in FR service; $E(Q(\boldsymbol{x},\boldsymbol{\xi}))$ is the expected value of the second-stage problem.

C. Deterministic Equivalence

Assuming $\boldsymbol{\xi}$ has a finite number of possible scenarios, denoted as $\boldsymbol{\xi}_1,\boldsymbol{\xi}_2,\ldots,\boldsymbol{\xi}_k$ with respective possibilities of $\rho_1,\rho_2,\ldots,\rho_k$, then the expectation form in (34) can be written as:

$$E(Q(\boldsymbol{x},\boldsymbol{\xi}))=\sum_{k=1}^{k_{\max}}\rho_k Q(\boldsymbol{x},\boldsymbol{\xi}_k) \tag{35}$$

Then, the original two-stage stochastic model can be formulated as the following deterministic equivalence:

$$\min_{\boldsymbol{x},\boldsymbol{y}_1,\boldsymbol{y}_2,\ldots,\boldsymbol{y}_k}\left\{f(\boldsymbol{x})+\sum_{k=1}^{k_{\max}}\rho_k g(\boldsymbol{x},\boldsymbol{y}_k)\right\} \tag{36}$$

s.t.

$$\boldsymbol{x}\in F \tag{37}$$

$$\boldsymbol{y}_k\in\Omega(\boldsymbol{x},\boldsymbol{\xi}_k)\quad\forall k \tag{38}$$

It can be seen from the formulation of optimization model that, at the first stage, a "here-and-now" decision $\boldsymbol{x}$ is made before the realization of the uncertain data $\boldsymbol{\xi}$ is known. Then, at the second stage, after a realization of uncertain scenario $\boldsymbol{\xi}$, a "wait-and-see" decision $\boldsymbol{y}$ is made to compensate for a possible inconsistency between the prediction and the reality at the first stage. In practice, the uncertain scenarios should be sampled from the probability distribution function of the uncertain variables, and the number needs to be reduced to a tractable number for solution.

Variables in the first-stage decision vector $\boldsymbol{x}$ are α_i, $t_{l,i}^{\mathrm{d,EA}}$, and $t_{l,i}^{\mathrm{d,FR}}$, which correspond to the selection for total service time and time spans of EA and FR services at the life stage l, respectively. The objective function in the first-stage problem is given as:

$$f(\boldsymbol{x})=\sum_{i=1}^{i_{\max}}\frac{1}{(1+r_{\mathrm{d}})^{\hat{t}_i^{\mathrm{Y}}}}C_{\mathrm{op,u}}\sum_{l=1}^{l_{\max}}\left(t_{l,i}^{\mathrm{d,EA}}+t_{l,i}^{\mathrm{d,FR}}\right) \tag{39}$$

Constraint set F corresponds to the constraints in (16)-(20) and (30)-(33).

In the second-stage decision, battery charging and discharging power in FR service is formulated according to the frequency deviations in each scenario. Variables in the second-stage decision vector are $P_{l,t_{\mathrm{EA}},i,k}^{\mathrm{EA,ch}}$ and $P_{l,t_{\mathrm{EA}},i,k}^{\mathrm{EA,dh}}$, which are the charging and discharging power of the BESS in EA service of each scenario, respectively. The objective function in the second-stage problem is given as:

$$g(\boldsymbol{x},\boldsymbol{y}_k)=-\sum_{i=1}^{i_{\max}}\frac{1}{(1+r_{\mathrm{d}})^{\hat{t}_i^{\mathrm{Y}}}}\left(\sum_{l=1}^{l_{\max}}t_{l,i}^{\mathrm{d,EA}}G_{l,i,k}^{\mathrm{EA}}+\sum_{l=1}^{l_{\max}}t_{l,i}^{\mathrm{d,FR}}G^{\mathrm{FR}}\right) \tag{40}$$

where $G_{l,i,k}^{\mathrm{EA}}$ and G^{FR} are calculated in (1) and (3), respectively.

Constraint set $\Omega(\boldsymbol{x},\boldsymbol{\xi}_k)$ corresponds to the constraints shown in (21)-(33). Based on the above analysis, the deterministic equivalence (36)-(38) is a mixed-integer nonlinear programming (MINLP) problem, which cannot be solved directly. The solution method used in this paper is shown in the next section.

V. Solution Method

A. Model Linearization

As $L_{l,t_{\mathrm{EA}},i}^{\mathrm{EA,ch}}$ and $L_{l,t_{\mathrm{EA}},i}^{\mathrm{EA,dh}}$ are calculated by the piecewise quadratic function in (14), $t_{l,i}^{\mathrm{d,EA}}L_{l,t_{\mathrm{EA}},i}^{\mathrm{EA,ch}}$ and $t_{l,i}^{\mathrm{d,EA}}L_{l,t_{\mathrm{EA}},i}^{\mathrm{EA,dh}}$ in (27)-(29) are highly nonlinear and make the optimization model difficult to be solved. A piecewise linear function is used to sim-

plify the function in (14). In the piecewise linear function, battery power is divided into several intervals with a series of breaking points. Then, a slope for each linear equation between the adjacent breaking points is calculated. Finally, the aging rate in (14) can be calculated by summing all the separated linear equations. Based on this linearization method, the highly nonlinear deterministic equivalent model is converted to a bilinear programming problem.

B. McCormick Envelopes and Bound Tightening Algorithm

McCormick envelopes and a bound tightening algorithm are used to solve the bilinear programming problem. Variable π and ω are used to present the bilinear items, i. e., $t_{l,i}^{\mathrm{d,EA}} G_{l,i}^{\mathrm{EA}}$ in (15), and $t_{l,i}^{\mathrm{d,EA}} L_{l,t_{\mathrm{EA}},i}^{\mathrm{EA,ch}}$ and $t_{l,i}^{\mathrm{d,EA}} L_{l,t_{\mathrm{EA}},i}^{\mathrm{EA,dh}}$ in (27)-(29). The auxiliary variable Γ is used to design the McCormick envelopes for the bilinear items:

$$\Gamma_u = \pi_u \omega_u \quad \forall u \tag{41}$$

McCormick envelopes are presented as:

$$\Gamma_u \geq \pi_u^{\min} \omega_u + \pi_u \omega_u^{\min} - \pi_u^{\min} \omega_u^{\min} \quad \forall u \tag{42}$$

$$\Gamma_u \geq \pi_u^{\max} \omega_u + \pi_u \omega_u^{\max} - \pi_u^{\max} \omega_u^{\max} \quad \forall u \tag{43}$$

$$\Gamma_u \leq \pi_u^{\min} \omega_u + \pi_u \omega_u^{\max} - \pi_u^{\min} \omega_u^{\max} \quad \forall u \tag{44}$$

$$\Gamma_u \leq \pi_u^{\max} \omega_u + \pi_u \omega_u^{\min} - \pi_u^{\max} \omega_u^{\min} \quad \forall u \tag{45}$$

A bound tightening algorithm is developed in Algorithm 1 to improve the performance of the solution method.

Algorithm 1: bound tightening algorithm

1: **Input**: tolerance $\xi(\xi>0)$, the maximum iteration number $\tau_{\max}$, parameters δ^0 and γ

2: **Initialize**: $\tau \leftarrow 0$; values for $\left(\pi_u^{\min}\right)^0$, $\left(\pi_u^{\max}\right)^0$, $\left(\omega_u^{\min}\right)^0$, and $\left(\omega_u^{\max}\right)^0$, which are initial limits of π_u and ω_u

3: **Repeat**

4: Solve convex optimization model by replacing the bilinear items with McCormick envelopes and obtain the results $\left(\pi_u^*\right)^\tau$, $\left(\omega_u^*\right)^\tau$ and $\left(\Gamma_u^*\right)^\tau$

5: $\left(\pi_u^{\min}\right)^{\tau+1} = \max\left\{(1-\delta^\tau)\left(\pi_u^*\right)^\tau, \left(\pi_u^{\min}\right)^0\right\}$

6: $\left(\pi_u^{\max}\right)^{\tau+1} = \min\left\{(1+\delta^\tau)\left(\pi_u^*\right)^\tau, \left(\pi_u^{\max}\right)^0\right\}$

7: $\left(\omega_u^{\min}\right)^{\tau+1} = \max\left\{(1-\delta^\tau)\left(\omega_u^*\right)^\tau, \left(\omega_u^{\min}\right)^0\right\}$

8: $\left(\omega_u^{\max}\right)^{\tau+1} = \min\left\{(1+\delta^\tau)\left(\omega_u^*\right)^\tau, \left(\omega_u^{\max}\right)^0\right\}$

9: $\delta^{\tau+1} = \gamma\delta^\tau, \tau \leftarrow \tau+1$

10: **Until** $\left|\left(\Gamma_u^*\right)^\tau - \left(\pi_u^*\right)^\tau\left(\omega_u^*\right)^\tau\right| \leq \xi\left|\left(\pi_u^*\right)^\tau\left(\omega_u^*\right)^\tau\right|, \forall u$ or $\tau \geq \tau_{\max}+1$

VI. Case Study

A. Parameter Settings

The proposed whole-lifetime coordinated service strategy is tested by a multifunctional BESS in EA and FR services. The NPV is used to evaluate the profit of BESS. The discount rate is 5% per year. The parameters of the BESS [22] and services [16], [29] are shown in Tables I and II, respectively. Life stages of the BESS [27] are defined in Table III. Cyclic aging characteristics [27] are shown in Fig. 2.

Calendar aging rate corresponding to the operation time at the life stage 1 κ_1^{cal} is 6.21×10^{-4} per day [22]. Calendar accelerating factors at different life stages χ_l are shown in Table IV [22].

TABLE I
Parameters of BESS

Parameter	Value
Rated energy capacity (MWh)	1
Rated power (MW)	1
Limits of stored energy (MWh)	[0.2,0.8]
Initial value of stored energy (MWh)	0.5
Charging/discharging efficiency η_c/η_d (%)	92
Maintenance cost ($/day)	20

TABLE II
Parameters of Services

Parameters	Value in EA service	Value in FR service
Time interval (s)	3600	1
Reserve price ($/MWh)		50
Reserve power (MW)		1
Δf_0 (HZ)		0.01
Δf_1 (HZ)		0.1
Power limit of BESS (MW)	[−1,1]	[−1,1]

TABLE III
Definition of Different Life Stages

Life stage l	SOH (%)
1	[100, 96]
2	[96, 87]
3	[87, 80]

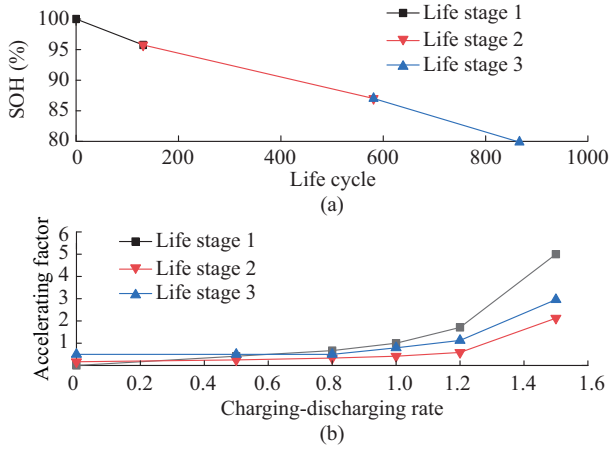

Fig. 2. Cyclic aging characteristics. (a) SOH variation when cycle depth is 100% and charging-discharging rate is 1. (b) Cyclic accelerating factor with different charging-discharging rates and life stages.

TABLE IV
Calendar Accelerating Factors

Life stage l	χ_l
1	1.000
2	0.483
3	0.298

According to the calendar aging parameters, the maximum stored time of the BESS is 10.17 years. Hence, the maximum time span of whole service period is set as 10 years, i.e., $\{\hat{t}_i^Y\}=\{1,2,\ldots,10\}$. The mean value and standard deviation of the historical electricity price [30] and frequency deviation [31] are shown in Fig. 3.

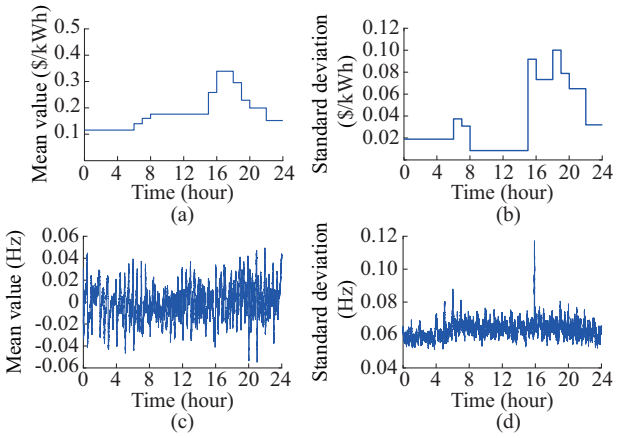

Fig. 3. Mean value and standard deviation of historical electricity price and frequency deviation. (a) Mean value of historical electricity price. (b) Standard deviation of historical electricity price. (c) Mean value of frequency deviation. (d) Standard deviation of frequency deviation.

The stochastic variations of predicted electricity price and frequency deviation are assumed to follow the normal distribution [32], [33]. Two hundred random scenarios are generated by Monte Carlo sampling to represent the stochastic variations of electricity price and frequency deviation. Then, the scenario reduction method in [34] is used to obtain 50 representative scenarios for stochastic programming.

The simulation is conducted on a 64-bit PC with 2.50 GHz CPU and 8 GB RAM, using Anaconda platform with Python 3.7.6 and GUROBI solver. The bilinear programming problem is solved by McCormick envelopes and the bound tightening algorithm in Algorithm 1.

B. Numerical Results

1) First-stage Decision Results

The first-stage decision results are shown in Fig. 4.

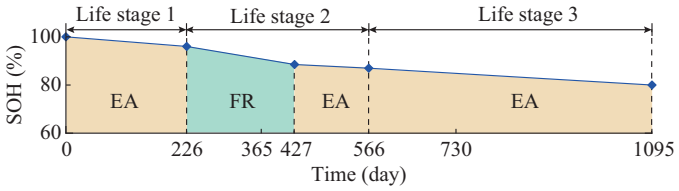

Fig. 4. First-stage decision results.

From Fig. 4, the optimal time span of the whole serve period is 3 years (1095 days). Life stage 1 of the BESS is from day 1 to day 226. Life stage 2 lasts from day 227 to day 566. Life stage 3 lasts from day 566 to day 1095. The proposed strategy switches the service from EA to FR on day 226 and then from FR to EA on day 427. The SOHs corresponding to the service switching points from EA to FR and from FR to EA are 96.00% and 88.50%, respectively. The BESS provides EA service at life stages 1, 2, and 3, and FR service at life stage 2. Using the proposed strategy, the whole-lifetime operation profit is $\$1.839\times10^5$.

Based on the above service strategy, the expected value of the operation profit and aging rate in each day at each life stage is shown in Table V. Based on the results in Table V, the per-degradation-rate operation profit at different life stages is shown in Fig. 5.

TABLE V
PROFIT AND AGING RATE AT DIFFERENT LIFE STAGES

Life stage	Expected value of operation profit ($)		Aging rate	
	EA	FR	EA	FR
1	1.546×10^2	5.800×10^2	2.657×10^{-4}	2.885×10^{-3}
2	1.585×10^2	5.800×10^2	2.412×10^{-4}	1.559×10^{-3}
3	1.533×10^2	5.800×10^2	4.764×10^{-4}	3.077×10^{-3}

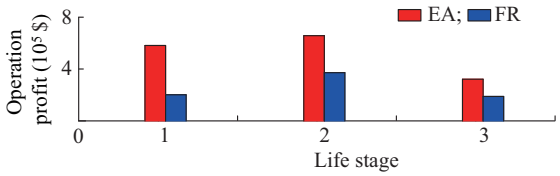

Fig. 5. Per-degradation-rate operation profit.

Based on the per-degradation-rate operation profit in Fig. 5 and the first-stage decision results in Fig. 4, the operation strategy selects the services with higher operation profits during the whole lifetime. Hence, the BESS provides EA services at life stages 1, 2, and 3, and FR service at life stage 2.

2) Second-stage Decision Results

For illustration purpose, typical scenarios shown in Fig. 6 are used as the input information to show the results in second-stage decision.

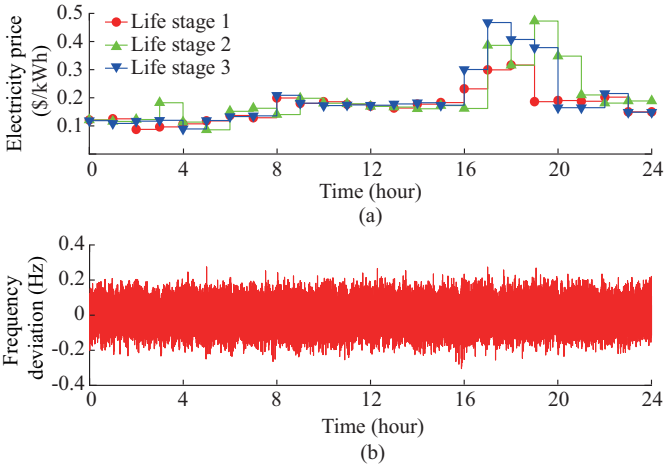

Fig. 6. Scenario information in second-stage decision. (a) Electricity price in EA service. (b) Frequency deviation in FR service at life stage 2.

The second-stage decision results in EA service are shown in Fig. 7. As can be observed from Fig. 7, the BESS is charged when the electricity price is low and discharged

when the electricity price is high. The SOC in EA service varies in a large range, whereas the power in EA service varies in a small range.

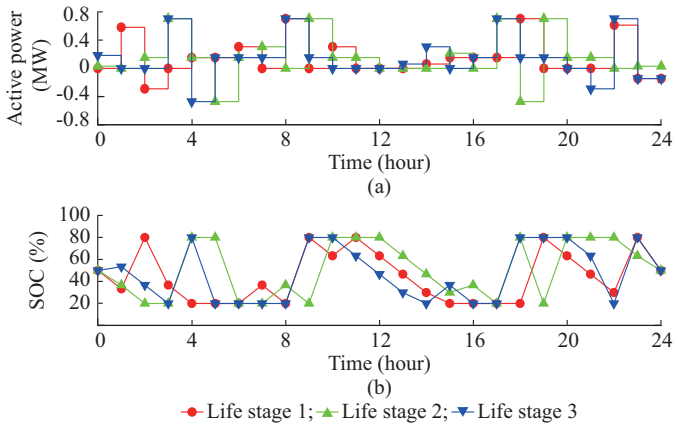

Fig. 7. Second-stage decision results in EA service. (a) Active power. (b) SOC.

The second-stage decision results in FR service at life stage 2 are shown in Fig. 8. From Fig. 8, in FR service, the BESS operates according to the frequency deviation during the regulation stages and operates in a constant power during the recovery stages. The SOC in FR service varies in a small range, whereas the power in FR service varies in a large range.

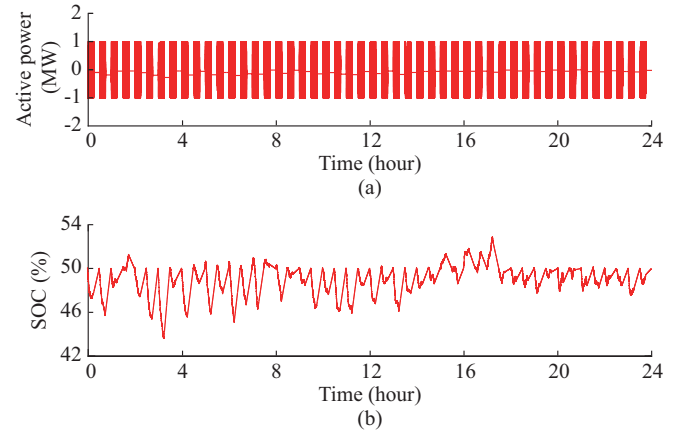

Fig. 8. Second-stage decision results in FR service. (a) Active power. (b) SOC.

C. Comparison with Single Service Strategies

The comparison with single service strategies is shown in Table VI.

TABLE VI
COMPARISON WITH SINGLE SERVICE STRATEGIES

Strategy	Optimal time span of whole service period (year)	Optimal operation profit (10^5 \$)
Proposed strategy	3	1.839
Single EA service strategy	4	1.742
Single FR service strategy	2	1.695

From Table VI, compared with the single EA and FR service strategies, the proposed strategy increases the operation profit by 5.57% and 8.50%, respectively.

D. Comparison with Existing Whole-lifetime Coordinated Service Strategy

The existing whole-lifetime coordinated service strategy divides the lifetime of a BESS into two stages [18]. The BESS provides FR service at the first stage and EA service at the second stage. These services are only switched once during the whole operation period. Multi-stage and calendar aging characteristics are ignored in the calculation of the aging rates [18]. Results using existing whole-lifetime coordinated service strategy are shown in Fig. 9.

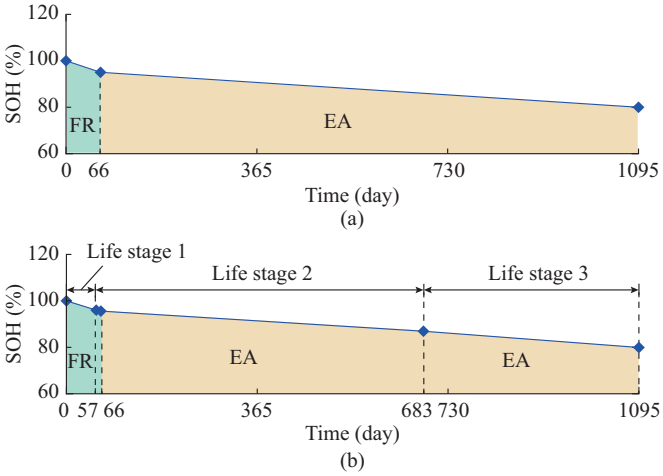

Fig. 9. Results using existing whole-lifetime coordinated service strategy. (a) Estimated SOH. (b) Actual SOH.

From Fig. 9, the optimal time span of whole service period is 3 years. The service is switched from FR service to EA service on day 66. The SOH corresponding to the service switching point is 95.61%. The actual operation profit using existing whole-lifetime coordinated service strategy is $\$1.658\times10^5$. Compared with the existing whole-lifetime coordinated service strategy, the proposed strategy increases the operation profit by 10.92%.

E. Analysis on Computation Time

The computation time of the proposed strategy is shown in Table VII.

TABLE VII
COMPUTATION TIME OF PROPOSED STRATEGY

Stage	Computation time (s)
First stage for service switching	453.910000
Second stage for EA service	1.420000
Second stage for FR service	0.000454

As can be observed from Table VII, the computation time to formulate the service switching decision for the whole lifetime is 453.91 s. As the service switching scheme is formulated before the operation of the BESS, the above computation time is acceptable in the practical application. The

computation time of the operation optimization in EA service is 1.42 s. As the battery power in EA service is formulated at the day-ahead stage, the above computation time is acceptable in the day-ahead optimization. The computation time for the formulation of battery power in FR service is 4.54×10^{-4} s. As the battery power in FR service is formulated every one second according to the frequency deviation, the above computation time is also acceptable in real-time application.

VII. Conclusion

Unlike previous works using the BESS to provide a single service or switch the service of the BESS only one time, this paper proposes a much more flexible whole-lifetime coordinated service strategy for BESSs. The proposed strategy switches the service of the BESS in EA and FR according to the battery aging characteristics at different life stages. Both external aging stress and internal reaction process are considered in the analysis on battery aging characteristics. A two-stage stochastic programming problem is formulated to optimize the proposed strategy. It is converted into an equivalent deterministic MINLP problem and solved using McCormick envelopes and a bound tightening algorithm. Testing results show that the proposed strategy can make full use of the battery aging characteristics. Compared with the existing single service strategies and whole-lifetime coordinated service strategies, the proposed strategy achieves the highest whole-lifetime operation profit.

With the development of battery modeling methods, the aging model in this paper can also be further improved to enhance the effectiveness of the proposed strategy. It should be noted that the proposed coordinated service strategy is not limited by the service modes or the number of life stages presented in this paper. For other service modes and other number of life stages, the proposed strategy can also formulate an optimal coordinated service scheme by including new service rules and new degradation properties. The research on other service modes and other numbers of life stages will be carried out in our future work.

References

[1] C. Zhang, Y. Xu, Z. Y. Dong *et al*., "Robust operation of microgrids via two-stage coordinated energy storage and direct load control," *IEEE Transactions on Power Systems*, vol. 32, no. 4, pp. 2858-2868, Jul. 2017.

[2] Y. Wang, Y. Xu, Y. Tang *et al*., "Aggregated energy storage for power system frequency control: a finite-time consensus approach," *IEEE Transactions on Smart Grid*, vol. 10, no. 4, pp. 3675-3686, Jul. 2019.

[3] A. A. Solomon, D. M. Kammen, and D. Callaway, "The role of large-scale energy storage design and dispatch in the power grid: a study of very high grid penetration of variable renewable resources," *Applied Energy*, vol. 134, pp. 75-89, Dec. 2014.

[4] S. Englberger, H. Hesse, N. Hanselmann *et al*., "SimSES multi-use: a simulation tool for multiple storage system applications," in *Proceedings of 2019 16th International Conference on the European Energy Market (EEM)*, Ljubljana, Slovenia, Sept. 2019, pp. 1-5.

[5] F. Fan, Y. Xu, and X. Feng, "Rule-based health-aware power sharing for a multi-unit battery energy storage system," *International Journal of Electrical Power & Energy Systems*, vol. 132, pp. 1-11, Nov. 2021.

[6] H. C. Hesse, V. Kumtepeli, M. Schimpe *et al*., "Ageing and efficiency aware battery dispatch for arbitrage markets using mixed integer linear programming," *Energies*, vol. 12, no. 6, pp. 1-28, Jan. 2019.

[7] G. Díaz, J. Gómez-Aleixandre, J. Coto *et al*., "Maximum income resulting from energy arbitrage by battery systems subject to cycle aging and price uncertainty from a dynamic programming perspective," *Energy*, vol. 156, pp. 647-660, Aug. 2018.

[8] D. Krishnamurthy, C. Uckun, Z. Zhou *et al*., "Energy storage arbitrage under day-ahead and real-time price uncertainty," *IEEE Transactions on Power Systems*, vol. 33, no. 1, pp. 84-93, Jan. 2018.

[9] B. Xu, Y. Shi, D. S. Kirschen *et al*., "Optimal battery participation in frequency regulation markets," *IEEE Transactions on Power Systems*, vol. 33, no. 6, pp. 6715-6725, Nov. 2018.

[10] X. Ke, D. Wu, and N. Lu, "A real-time greedy-index dispatching policy for using PEVs to provide frequency regulation service," *IEEE Transactions on Smart Grid*, vol. 10, no. 1, pp. 864-877, Jan. 2019.

[11] P. Denholm, J. Jorgenson, M. Hummon *et al*. (2013, May). Value of energy storage for grid applications. [Online]. Available: https://www.osti.gov/biblio/1079719

[12] M. Kazemi, H. Zareipour, N. Amjady *et al*., "Operation scheduling of battery storage systems in joint energy and ancillary services markets," *IEEE Transactions on Sustainable Energy*, vol. 8, no. 4, pp. 1726-1735, Oct. 2017.

[13] Y. Shi, B. Xu, D. Wang *et al*., "Using battery storage for peak shaving and frequency regulation: joint optimization for superlinear gains," *IEEE Transactions on Power Systems*, vol. 33, no. 3, pp. 2882-2894, May 2018.

[14] B. Cheng and W. B. Powell, "Co-optimizing battery storage for the frequency regulation and energy arbitrage using multi-scale dynamic programming," *IEEE Transactions on Smart Grid*, vol. 9, no. 3, pp. 1997-2005, May 2018.

[15] X. Li, R. Ma, W. Gan *et al*., "Optimal dispatch for battery energy storage station in distribution network considering voltage distribution improvement and peak load shifting," *Journal of Modern Power Systems and Clean Energy*, vol. 10, no. 1, pp. 131-139, Jan. 2022.

[16] P. H. Divshali and C. Evens, "Optimum operation of battery storage system in frequency containment reserves markets," *IEEE Transactions on Smart Grid*, vol. 11, no. 6, pp. 4906-4915, Nov. 2020.

[17] Australian Energy Market Operator. (2018, Jun.). Managing frequency in the power system. [Online]. Available: https://aemo.com.au/learn/energy-explained/energy-101/managing-frequency-in-the-power-system

[18] Y. Zhang, Y. Xu, H. Yang *et al*., "Optimal whole-life-cycle planning of battery energy storage for multi-functional services in power systems," *IEEE Transactions on Sustainable Energy*, vol. 11, no. 4, pp. 2077-2086, Oct. 2020.

[19] L. Cheng, Y. Wan, Y. Zhou *et al*., "Operational reliability modeling and assessment of battery energy storage based on Lithium-ion battery lifetime degradation," *Journal of Modern Power Systems and Clean Energy*. doi: 10.35833/MPCE.2021.000197

[20] U. C. Yilmaz, M. E. Sezgin, and M. Gol, "A model predictive control for microgrids considering battery aging," *Journal of Modern Power Systems and Clean Energy*, vol. 8, no. 2, pp. 296-304, Mar. 2020.

[21] Y. Gao, X. Zhang, B. Guo *et al*., "Health-aware multiobjective optimal charging strategy with coupled electrochemical-thermal-aging model for lithium-ion battery," *IEEE Transactions on Industrial Informatics*, vol. 16, no. 5, pp. 3417-3429, May 2020.

[22] B. Xu, A. Oudalov, A. Ulbig *et al*., "Modeling of Lithium-ion battery degradation for cell life assessment," *IEEE Transactions on Smart Grid*, vol. 9, no. 2, pp. 1131-1140, Mar. 2018.

[23] V. Kumtepeli, H. C. Hesse, M. Schimpe *et al*., "Energy arbitrage optimization with battery storage: 3D-MILP for electro-thermal performance and semi-empirical aging models," *IEEE Access*, vol. 8, pp. 204325-204341, Nov. 2020.

[24] U. Akram, M. Nadarajah, R. Shah *et al*., "A review on rapid responsive energy storage technologies for frequency regulation in modern power systems," *Renewable and Sustainable Energy Reviews*, vol. 120, p. 109626, Mar. 2020.

[25] T. R. Tanim and C. D. Rahn, "Aging formula for lithium ion batteries with solid electrolyte interphase layer growth," *Journal of Power Sources*, vol. 294, pp. 239-247, Oct. 2015.

[26] X. Han, M. Ouyang, L. Lu *et al*., "A comparative study of commercial lithium ion battery cycle life in electrical vehicle: aging mechanism identification," *Journal of Power Sources*, vol. 251, pp. 38-54, Apr. 2014.

[27] Y. Gao, J. Jiang, C. Zhang *et al*., "Lithium-ion battery aging mechanisms and life model under different charging stresses", *Journal of Power Sources*, vol. 356, pp. 103-114, Jul. 2017.

[28] J. Schmalstieg, S. Käbitz, M. Ecker *et al*., "A holistic aging model for Li (NiMnCo) O_2 based 18650 Lithium-ion batteries," *Journal of Power Sources*, vol. 257, pp. 325-334, Jul. 2014.

[29] A. Oudalov, D. Chartouni, and C. Ohler, "Optimizing a battery energy

storage system for primary frequency control," *IEEE Transactions on Power Systems*, vol. 22, no. 3, pp. 1259-1266, Aug. 2007.
[30] J. Schofield, "Dynamic time-of-use electricity pricing for residential demand response: design and analysis of the low carbon london smart-metering trial," Ph.D. dissertation, Department of Electrical and Electronic Engineering, Imperial College London, London, UK, 2015.
[31] National Grid ESO. (2021, Jan.). Frequency response service. [Online]. Available: https://www. nationalgrideso. com/balancing-services/frequency-response-services/historic-frequency-data
[32] J. Engels, B. Claessens, and G. Deconinck, "Combined stochastic optimization of frequency control and self-consumption with a battery," *IEEE Transactions on Smart Grid*, vol. 10, no. 2, pp. 1971-1981, Mar. 2019
[33] Z. Chen, L. Wu, and Y. Fu, "Real-time price-based demand response management for residential appliances via stochastic optimization and robust optimization," *IEEE Transactions on Smart Grid*, vol. 3, no. 4, pp. 1822-1831, Dec. 2012.
[34] Y. Xu, Z. Y. Dong, R. Zhang *et al*., "Multi-timescale coordinated voltage/var control of high renewable-penetrated distribution systems," *IEEE Transactions on Power Systems*, vol. 32, no. 6, pp. 4398-4408, Nov. 2017.

Feilong Fan received the B.E. degree in electrical engineering from Zhejiang University, Hangzhou, China, in 2014, and Ph.D. degree in electrical engineering from Shanghai Jiao Tong University, Shanghai, China, in 2019. He is currently a Research Fellow in Nanyang Technological University, Singapore. His research interests include energy management of distribution systems, micro grid, and battery storage systems.

Yan Xu received the B.E. and M.E degrees from South China University of Technology, Guangzhou, China, in 2008 and 2011, respectively, and the Ph. D. degree from The University of Newcastle, Newcastle, Australia, in 2013. He conducted postdoctoral research with the University of Sydney Postdoctoral Fellowship, Sydney, Australia, and then joined Nanyang Technological University (NTU) with The Nanyang Assistant Professorship, Singapore. He is now an Associate Professor at School of Electrical and Electronic Engineering and a Cluster Director at Energy Research Institute @ NTU (ERI@N), Singapore. He is an Editor for IEEE Transactions (TSG and TPWRS), IET Journals (GTD and ECE), and China's power engineering international journals (MPCE and CSEE JPES). He is also serving as the Chairman for IEEE Power & Energy Society Singapore Chapter. His research interests include power system stability and control, microgrid, and data-analytics for smart grid applications.

Rui Zhang received the B. E. degree from the University of Queensland, Brisbane, Australia, and the Ph.D. degree from the University of Newcastle, Newcastle, Australia, in 2009 and 2014, respectively. She is now with University of New South Wales, Sydney, Australia. Her research interests include power system operation, control, and stability.

Tong Wan received the B.E. degree from Queensland University of Technology, Brisbane, Australia, and the M. E degree from the University of Sydney, Sydney, Australia, in 2007 and 2021, respectively. Her research interests include energy storage and renewable energy planning and risk management.